Review of High-Precision Sr Isotope Analyses of Low-Sr Geological Samples

Jie Lin, **Yongsheng Liu***, **Haihong Chen**, **Lian Zhou**, **Zhaochu Hu**, **Shan Gao**
State Key Laboratory of Geological Processes and Mineral Resources, China University of Geosciences, Wuhan 430074, China

ABSTRACT: Isotope plays an important role in both tracing and dating in earth science, especially ^{87}Rb-^{86}Sr system. With the development of earth science, whole-rock analysis can't sufficiently meet the requirements for scientific research and the micro-analysis becomes more and more significant. Laser ablation multi-collector inductively-coupled plasma mass-spectrometry (LA-MC-ICP-MS) has been extensively applied in micro-zone analysis due to its low sample-consumption, high accuracy, in situ and low requirements on matrix, but it is still difficult to accurately measure Sr isotope compositions especially for the samples with high Rb/Sr ratios and low Sr contents as it is restricted by severe quality discrimination and various types of mass spectrum interferences. Consequently, thermal ionization mass-spectrometry (TIMS), as the most accurate and precise method to analyze isotopic ratios, is still the most popular method of analyzing Sr ratios, especially for the samples with low Sr contents. This paper makes a systematic review on the high-precision Sr isotope analyses of low-Sr geological samples, including the micro-sampling technique, ultra-low procedural blank chemical method and TIMS measurement technique. The combination of ultra-low procedural blank and TIMS can be used to perform high-precision micro-analysis of the samples with ng magnitude, which will be undoubtedly an important direction for Rb-Sr geochronology, geochemistry and environmental studies.
KEY WORDS: Sr isotope compositions, Ultra-low procedural blank, TIMS, Micro-sampling, Sr-specific resin, Micro-ion exchange column.

0 INTRODUCTION

Since the Mid-20th century, ^{87}Rb-^{86}Sr isotope dating and Sr isotope geochemistry tracing have been widely used in earth science, astrochemistry, archeology and environmental science and other fields (Maxwell and Culligan, 2009; Komárek et al., 2008; Font et al., 2007; Tong et al., 2006; Dickin, 2005). Compared with the traditional methods of grinding and dissolving the entire sample, high-precision microanalysis can reveal the internal heterogeneity of samples and provide better support for geological interpretation. For example, the measurement of the micro-element and isotope ratios in crystal core and margin can be used to study the environmental change during crystal growth process and explore its important geological significance such as crust-mantle contamination or replenishment of magma.

Currently, there are two methods for Sr isotope microanalysis: micro-sampling-thermal-ionization mass spectrometry (TIMS) and laser ablation multi-collector inductively coupled plasma mass spectrometry (LA-MC-ICP-MS), among which, LA-MC-ICP-MS has been extensively used in Sr isotope micro-analysis due to its small sample-consumption, high precision, in-situ and low requirements on matrix (Konter and Storm, 2014;

Kimura et al., 2013; Jochum et al., 2009; Waight et al., 2002). However, there are three major limitations to measure in-situ Sr isotope ratios by LA-MC-ICP-MS. Firstly, severe mass-dependent fractionation of Sr element will occur during the process of laser ablation, aerosol transmission and mass analysis (Liu et al., 2013; Mank and Mason, 1999); Secondly, Rb, Ca argides and Ca dimers (Waight et al., 2002), doubly charged REE and the trace Kr（^{84}Kr and ^{86}Kr）existed in ICP work gas (Ar) will produce spectral interference on Sr; Finally, it is difficult to high-precision analyze Sr isotope ratios of the minerals with low Sr content due to the small volume sampled by laser ablation. These factors make LA-MC-ICP-MS be incompetent to measure Sr isotope in minerals with low Sr contents <30 ppm (Jochum et al., 2009). Although Kimura et al. (2013) and Konter and Storm (2014) have improved the correction method of Kr, it remains difficult to eliminate large error brought by the signal instability of Kr and iterative computation. TIMS is still the best choice to measure Sr isotope ratios of samples after being dissolved and purified, especially for the minerals with high Rb contents (such as mica and feldspar), (Raddatz et al., 2013; Chu et al., 2009; Yokoyama and Nakamura, 2004; Deniel and Pin, 2001). For the traditional sample dissolution method, the sample mass is generally greater than 50 mg due to be restriced by instrumental performance and procedural blank (Li et al., 2012), which may result in the mixture of multi-phase minerals. Thus, only by reducing the mass needed can we get the accurate Sr isotope ratios of trace monomineral, which should reduce procedural blank and improve the

instrument performance. In summary, there are three necessary conditions to realize the in situ analysis of the Sr isotope compositions in minerals with low Sr contents, including micro-sampling, ultra-low procedural blank, trace Sr isotope ratios analysis by TIMS.

At present, the micro-sampling is generally accomplished by micro-drilling and laser ablation in liquid (LAL). Micro-drilling sampling technique can get almost non-polluting micro-sampling on sample surface using tungsten carbide bit (Charlier et al., 2006), but its spatial resolution is limited by sample diameter (about 0.2 mm) and depth (about 1 mm). For the LAL technique, the sample volume can be controlled by changing laser conditions (Barcikowski et al., 2007; Besner et al., 2007; Kabashin and Meunier, 2007). Claverie et al. (2013) proved that this method was free from severe elemental and isotopic fractionation. Compared with traditional Sr cation exchange resin (Dowe 50 type and AG 50 type) (Li et al., 2011; Raczek et al., 2003; Na et al., 1995), the development and utilization of Sr spec^{TM} resin can not only reduce acid amount and procedural blank, but also be efficient to the separate Ca, Ba and Rb from Sr, which has significantly promoted the development of Sr isotope analysis (Wall et al., 2013; Font et al., 2007; Charlier et al., 2006; Li et al., 2005; Philip Horwitz et al., 1992). Many scholars have designed the micro-exchange column applicable to micro-sample separation (Harlou et al., 2009; Font et al., 2007; Charlier et al., 2006). In addition, the separation device was optimized by adding the vacuum system (Wall et al., 2013). Additionally, further improvements in sample loaded method and instrumental parameters are needed to obtain precise data (Font et al., 2012; Harvey and Baxter, 2009; Harlou et al., 2009; Charlier et al., 2006).

In summary, great progresses and rapid developments have been achieved in separating and determining the Sr isotope ratios of the samples with low Sr contents. This paper has systematically summarized the acquired achievements in measuring the Sr isotope ratios of the samples with low Sr contents by ultra-low procedural blank chemical separation process combined with TIMS, aiming at further promoting the research and applications of this method.

1 SOURCES, MEASUREMENT AND CORRECTION OF Sr PROCEDURAL BLANK

Total procedural blank (mass of the analyzed elements of blank samples) is generally used to evaluate the procedural blank of the whole experiment (Košler and Magna, 2014). For the samples with low Sr content, it is generally required that the blank value should be 0.1%–0.01% of sample content (Charlier et al., 2006). Procedural blank is predominantly derived from sample preparation process.

1.1 Sources of Sr Procedural Blank

In order to reduce the blank of laboratory environment, experiments should be performed in the laboratory equipped with high-efficiency particulate air (HEPA)-filtered laminar airflow (Košler and Magna, 2014; Hu and Qi, 2014; Wall et al., 2013; Fortunato et al., 2004). In addition, much more attention should be paid attention to laboratory materials (polypropylene and polytetrafluoroethylene, etc.,), temperature (~20 °C), pressure (higher than outdoor 5–30 Pa) and humidity (40%–50%) (Moody and Lindstrom, 1977). To some extent, the specifically used HEPA-filtered box and clean containers can reduce procedural blank (Harlou et al., 2009; Hinn and Nelson, 1997).

Clean containers that are not easy to result in penetration and contamination are necessary to be used for ultra-low procedural blank chemical process. It has been reported that the contributions of the vessels made by different materials on procedural blank generally follow such order: low-density polyethylene <fluorocarbons<synthetic quartz <high density polyethylene <natural quartz <platinum <borosilicate (Hu and Qi, 2014). Additionally, Reimann et al. (2010) reported that dark-colored containers leach more materials than clear containers do for most elements, and this observation is independent of the container material.

Resin is the major source of procedural blank (Harlou et al., 2009; Charlier et al., 2006) (Fig. 1). Thereby, the Sr spec^{TM} resin should be pre-cleaned by a large amount of acid before
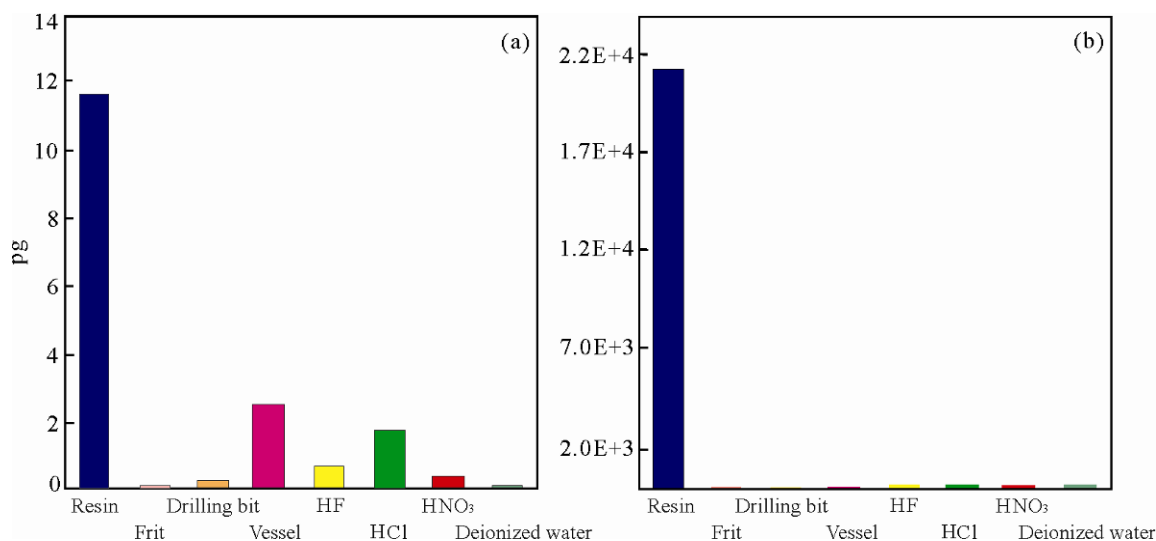

Figure. 1 Blank of Rb (a) and Sr (b) in vessels, reagents and resins (Harlou et al., 2009).

being used or after being loaded in micro-exchange column. For example, Charlier et al. (2006), Font et al. (2007) and Harlou et al. (2009) used a lot of HCl and deionized water to pre-clean Sr spec^{TM} resin and 6 L acid solution (0.05 N HNO$_3$+0.1 N H$_2$SO$_4$+6NHCl) to clean the 70 μL Sr spec^{TM} resin that are loaded in micro-exchange column.

The procedural blank will be influenced by reagent types, volume and degree of purification (Jackson et al., 1992). In order to reduce the reagent blank, firstly, the reagent should be as pure as possible, such as the ultra-pure reagents produced by Seastar Chemicals^{TM} Company used by Charlier et al. (2006). Secondly, the reagent volume should be as small as possible, for example, Font et al. (2007) and Harlou et al. (2009) only used approximately 1 ml reagent to perform chemical separation. Finally, reagent purification times should be as many as possible and purification mode should be optimized (Hu et al., 2005). For example, Li et al. (2011) distilled and purified the HF, HCl and HNO$_3$ (MOS level) four times using PFA sub-boiling distillation. The metal cation in reagent can be removed by distillation (Yuan et al., 2000; Kuehner et al., 1972), but it is not the fact that the more the distillation frequency is, the lower the reagent blank is (Hinn and Nelson, 1997). In addition, as the purity of water directly affects procedural blank, the deionized water with a temperature of 25 °C, pH of 7 and resistivity of 18.2 MΩ·cm should be finally obtained (Košler and Magna, 2014). It should be noted that the deionized water after a filter change generally has a high content of Rb-Sr (Harlou et al., 2009).

1.2   Measurement and Correction of Sr Procedural Blank
1.2.1   Measurement of Sr procedural blank

The element content and isotopic ratio of the procedural blank (Hwang and Druffel, 2008) as well as the estimation on their error (Košler and Magna, 2014) should be measured. The higher accuracy of the estimation of the element content and isotopic ratio is, the smaller the error resulted from procedural blank correlation (Fig. 2). The measurement accuracy is positively correlated with element content (Košler and Magna, 2014; Lin et al., 2014; Hu et al., 2012), thus, the multiple samples with procedural blank obtained under the same conditions are generally amalgamated. The following two methods are typically applied to measure element content: ① Applying Q-ICP-MS or HR-ICP-MS to measure the Sr concentration of blank solution, then obtaining the mass of Sr in procedural blank according to solution mass (Harlou et al., 2009; Font et al., 2007); ② Applying isotope dilution method (ID)-TIMS to measure the mass of Sr procedural blank.

1.2.2   Correction of Sr procedural blank

For the samples with high Sr contents (> 20 ng) (Košler and Magna, 2014), the influence of procedural blank on the isotope ratio is almost negligible (Charlier et al., 2006), but the blank must be corrected if the element content is low or the isotope ratio of procedural blank is largely different from that of sample. The procedural blank can be corrected as follows (Hayes, 1983):

$$r_{sam} = \frac{r_{sam+blk} \times m_{sam+blk} - r_{blk} \times m_{blk}}{m_{sam+blk} - m_{blk}} \qquad (1.1)$$
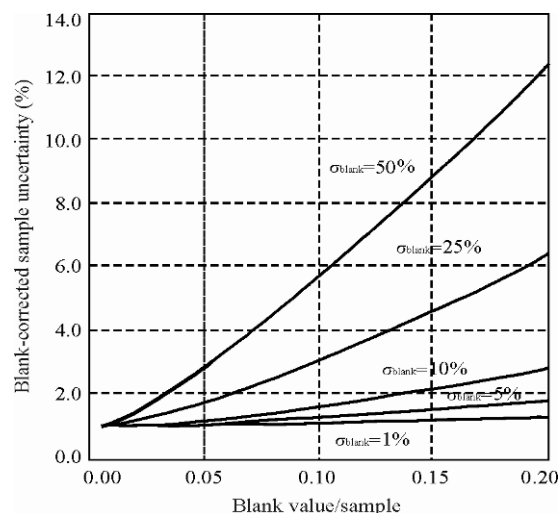

Figure. 2 Relationship between procedural blank, uncertainty of blank measurement and final error of sample measurement (Modified from Košler and Magna, 2014).

Here, m_{blk} and $m_{sam+blk}$ are the Sr mass of procedural blank and sample after being separated and purified, respectively; r_{blk} and $r_{sam+blk}$ are the $^{87}Sr/^{86}Sr$ of procedural blank and sample after being separated and purified, respectively; r_{sam} is the real isotope ratio of the sample after blank correction. r_{sam} can be easily calculated when the first four data are known. With the Sr blank correction method, Harlou et al. (2009) obtained the isotope ratio with accuracy increased by about 2 518 ppm.

Hwang and Druffel (2008) proposed to convert Eq. 1.1 to Eq. 1.2 when the procedural blank of carbon element was corrected, and then they performed separation measurements of the same sample with different element contents using the same experimental procedure and obtained a linear relationship between $1/(m_{blk}+m_{sam})$ and $r_{sam+blk}$, where, the intercept of the line r_{sam} is the isotope ratio of samples after blank correction.

$$r_{sam+blk} = r_{sam} + (r_{blk} - r_{sam})m_{blk} \times \frac{1}{m_{blk} + m_{sam}} \qquad (1.2)$$

In addition, since the element content of procedural blank is low, the measurement error of element content and isotope ratio is large. Hwang and Druffel (2008) proposed to apply standard dilution method to obtain $m_{blk} \times r_{blk}$ indirectly, which was calculated through the standards before and after purification and separation. Eq. 1.2 can be converted to Eq. 1.3.

$$r_{sam} = \frac{r_{sam+blk} \times m_{sam+blk} - \left[r_{std+blk} \times m_{std+blk} - r_{std}(m_{std+blk} - m_{blk}) \right]}{m_{sam+blk} - m_{blk}} \qquad (1.3)$$

Here, $r_{std+blk}$ and $m_{std+blk}$ represent the isotope ratios and element mass of the standards after separation and purification, r_{std} represents the isotope ratio of standards before separation and purification.

$$\left[r_{std+blk} \times m_{std+blk} - r_{std}(m_{std+blk} - m_{blk}) \right] \text{is} \quad m_{blk} \times r_{blk} \qquad (1.4)$$

2   SAMPLE PREPARATION

2.1   Micro-Sampling

Typical micro-sampling methods include micro-drilling sampling (Arslan and Secor, 2008; Font et al., 2007; Charlier et al., 2006; Müller et al., 2000a; Müller et al., 2000b) and laser ablation sampling in which samples are placed in deionized water (Okabayashi et al., 2011).

Prior to micro-drilling sampling, the location of samples should be determined by SEM to avoid fractures or impurities (Müller et al., 2000b). Sr content of the samples can be measured by LA-ICP-MS or electron probe to predetermine the sample volume (Arslan and Secor, 2008). In order to avoid the cross-contamination during sample collection, the sample surface should be tightly pressed with a sealing film and dropped with one drop of high purity water. Then, micro-sampling can begin after parameters such as drilled depth are setted according to sample volume. The obtained turbid liquid of samples should be transferred into a clean container using a clean pipette, and then poured into acetone, alcohol and deionized water to ultrasonically clean and weighed using a balance (Košler and Magna, 2014). Charlier et al. (2006) demonstrated that micro-drilling device can realize no-polluting sampling from a small amount of samples. Currently, the device has been successfully used in fish otoliths (Arslan and Secor, 2008), carbonate rocks (Hoffmann et al., 2009), clinopyroxene (Charlier et al., 2006) and graphite (Chen et al., 2010).

Commonly, the laser device used for laser ablation in liquid is the titanium jewel femtosecond laser with fundamental wavelength of 800 nm, and the liquid used is the deionized water with low vapor pressure, low blank and low absorption amount of 800 nm beam (Okabayashi et al., 2011). Samples are placed in deionized water, about 2 mm away from the water surface. The small particles obtained by laser ablation can form nanoparticle suspension (Fig. 3), which can be cleaned and weighted according to the mentioned micro-sampling process. Okabayashi et al. (2011) had measured the $^{238}U/^{232}Th$, $^{208}Pb/^{206}Pb$ of NIST SRM 610 and $^{56}Fe/^{54}Fe$, $^{57}Fe/^{57}Fe$ of IRMM-014, and the obtained results were consistent with recommended values with an error range of <0.5%. This method has the following advantages: (1) the sample particles generated by laser ablation are very small. For example, the particles obtained by Kabashin and Meunier (2007) is about 6–15 nm. Hence, the dissolution time of samples can be greatly shortened; (2) The sampling amount can be well controlled and the spatial resolution can be improved by optimizing laser wavelength (Okabayashi et al., 2011), frequency, energy density (Kabashin and Meunier, 2007) and ablation time (Besner et al., 2007); (3) The blank generated by LA is lower than that by micro-sampling; (4) The elemental fractionation and isotopic fractionation are within errors of instrumental measurement (Okabayashi et al., 2011).

2.2   Sample Digestion

The commonly used dissolution methods include alkali fusion method, resolution microwave digestion method, open-acid dissolution method and high-pressure closed acid digestion method. The samples with low Sr content in this paper are feldspar, garnet and mica, and the commonly used methods are
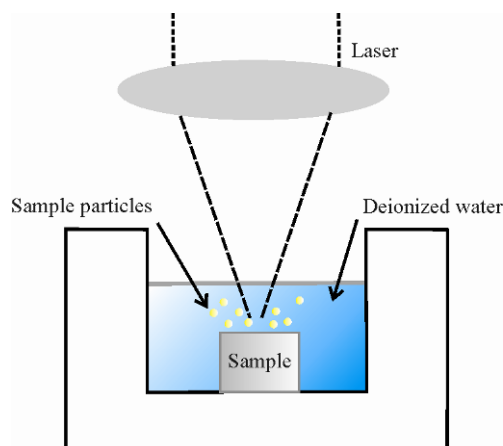

Figure. 3 Schematic diagram of experimental setup for LA. Samples are placed in the deionized water about 2 mm underneath from the surface(Okabayashi et al., 2011).

open-acid digestion method (Harlou et al., 2009; Font et al., 2007; Charlier et al., 2006) and high-pressure steam dissolution method (Li et al., 2005).

The commonly used acid combination is $HF/HClO_4$ and HF/HNO_3 etc (Hu and Qi, 2014; Jarvis, 1990). For open-acid digestion method, the procedural blank and the loss of some elements will increase because the containers are open and large volume of acid is used during the dissolution process. Some elements in insoluble minerals have extremely low recovery because the maximum dissolution temperature is restricted by the low acid boiling point (Hu and Qi, 2014). The insoluble minerals almost can be completely dissolved by the high-pressure closed acid digestion method. However, the use of HF will lead to the formation of insoluble fluoride precipitation (Yokoyama et al., 1999; Boer et al., 1993). For Rb-Sr isotopic system, Sr is easy to precipitate due to its low solubility in HF, while Rb is easy to form fluoride co-precipitation with major elements (Langmyhr, 1967). Several ways can prevent fluoride from precipitating, e.g. reducing the dissolved sample amount (Hu and Qi, 2014; Hu et al., 2010), adding $HClO_4$ during sample dissolution process (Navarro et al., 2008) or incompletely evaporating acid-dissolving samples (Cotta and Enzweiler, 2012; Hu et al., 2010; Navarro et al., 2008; Dulski, 2001). Rock samples also can be dissolved using a combination of NH_4F and HNO_3 (Hu et al., 2010; Mariet et al., 2008). Moreover, Zhang et al. (2012) developed a method that dissolved rock samples using NH_4HF_2 (239.5 °C). Applying NH_4F or NH_4HF_2 to replace HF can not only reduce laboratory safety risks to a certain extent, but also decrease reagent volume.

In the sample dissolution method with high-pressure steam , $HF+HNO_3$ and sample dissolving cup are placed at the bottom of enclosed stew pot and carrier table, respectively. In addition, sample dissolving acid ($HF+HNO_3$) and samples are not mixed to heat together to decrease the blank brought by the used acids (the Sr blank for this method is generally 2 pg) (Li et al., 2005). The monomineralic samples (mainly feldspar, garnet, mica, etc.) extracted from micro-drilling can be completely dissolved by this method.

Table 1 lists the different sample dissolution methods used

by different researchers.

2.3   Sample Separation and Enrichment

TIMS puts an extreme demand on element purity, so the interference elements in samples must be removed. For Sr isotope, the main interference elements are Rb, Ca, Ba and other major elements. ^{87}Rb is the isobar of ^{87}Sr, which can't be distinguished from ^{87}Sr by the existing mass spectrometer due to its low resolution (De Muynck et al., 2009; Galler et al., 2007).

Ca, Ba and Sr belong to the same major group and their ionic radius is similar, which are difficult to be completely separated with each other by traditional cationic resin. The accurate determination of Sr isotope can be seriously influenced by Ca because the residual Ca will seriously halt Rb depleted on the metal filament (De Muynck et al., 2009; Dickin, 2005). Sr spec ^{TM} resin can separate Sr from Ca and Ba completely (Scher et al., 2014; Palmer et al., 2000; Philip Horwitz et al., 1992) (Fig. 4).

Table 1   Comparison of different sample dissolution methods

Number	Sample dissolving steps	Reference	Note
1	① Using 200 μl 29 N HF and 10 μl 10 N HNO$_3$ to dissolve 3.75 μg samples in Savilex open sample dissolving c; ② Tightening the lid and heating (80 °C) for 24h under sealing conditions; ③ Evaporating the solution to dryness and removing redundant HF and the SiF$_4$ generated ④ Adding 200 μl 6 N HCl and heating for several hours under sealing conditions; ⑤ Evaporating the solution to dryness, adding 10 N HNO$_3$ and heating for several hours under sealing conditions; ⑥ Evaporating the samples to dryness, adding 200 μl 3 N HNO$_3$ and heating under sealing conditions to reserve.	(Charlier et al., 2006)	Open acid sample dissolving method can dissolve samples completely, but needs long experimental time.
2	① Placing 2 ml HF + 0.2 ml HNO$_3$ and sample dissolving cup on sealed stew cans and carrier table, then heating for 48h in 195 °C constant temperature oven; ② Taking out the sample dissolving cup and removing redundant HF acid, then adding 0.1 ml 3N HNO$_3$ and evaporating to dryness again; ③ Cooling to room temperature, then adding 200 μl 3N HNO$_3$ to reserve.	(Li et al., 2005)	Steam sample dissolving method can dissolve samples rapidly.
3	① Weighting 50 mg rock samples and 500 mg NH$_4$F in Teflon breaker, and adding 1 ml HNO$_3$. Placing Teflon breaker in stainless steel sleeve, then heating for 24 h in 190 °C heating furnace under sealed conditions; ② Opening the lid, heating to near dryness state on 120 °C heating plate, then adding 1 ml HNO$_3$ and evaporating to dryness. Dissolving the samples with 1.5 ml and 2.5 ml ultrapure water; ③ Placing Teflon breaker into stainless steel sleeve again, and heating overnight at a temperature of 150 °C under sealed conditions.	(Hu et al., 2010)	NH$_4$F and NH$_4$HF$_2$ method can dissolve samples completely, but it has not been used for isotope test yet.
4	① Weighting 200 mg NH$_4$HF$_2$ and 50 mg rock powder in the Teflon breakers ; ② Tightening the lid and heating for 3h in 230 °C heating furnace; ③ After cooling, adding 2 ml HNO$_3$ into breaker, tightening the lid and heating for 1h on 160 °C heating plate. Opening the lid and heating to dryness state on 60 °C heating plate; ④ Adding 1 ml HNO$_3$ and 1 ml ultrapure water into samples. Tightening the lid and heating for 5h on heating plate.	(Zhang et al., 2012)	

Sr spec ^{TM} resin is obtained from 4, 4 '(5') -2-3-cyclohexyl and 18-crown-6 (crown ether) (Fig. 5) that coated on an inert carrier in octanol. Its metal ion separating ability depends on the matching degrees between crown ether ring and metal ion (radius and ligand orientation). The Sr^{2+} with diameter of 22.4 nm can just be wrapped by the crown ether cavity with diameter of 26–32 nm, thus, it has specific selectivity for Sr^{2+}. The combining capacity between metal ion and Sr special resin varies with nitric acid concentration (Wall et al., 2013; Philip Horwitz et al., 1992), the larger the HNO$_3$ concentration is used, the greater the combining capacity between Sr and Sr spec^{TM} resin is and the greater the distribution coefficient is, for example, the distribution coefficient of Sr is up to about 100, whereas the distribution coefficient of other metal ions is small when the concentration of HNO$_3$ is 8 N, while the distribution coefficient of Sr is only 1

when the HNO$_3$ concentration is 0.05 N. So the interference elements can be separated by 8 N HNO$_3$, while the Sr can be collected by 0.05 N HNO$_3$ or deionized water (Fig. 6) (Scher et al., 2014; Harlou et al., 2009). Furthermore, it has been reported that Sr spec^{TM} resin represented the best selectivity only when the milliequivalents of samples were not more than 0.1 times of resin (Palmer et al., 2000; Philip Horwitz et al., 1992). Among which, Sr spec ^{TM} resin has a density of 0.33 g/ml and 1 g resin can separate 27 mg Sr. The Sr recovery is generally less than 100% when Sr spec^{TM} resin is used because some Sr will run off during eluting interference elements and some Sr will remain in resin since Sr is closely contacted with Sr spec^{TM} resin (Charlier et al., 2006). Wall et al. (2013) proved that mass fractionation of Sr could be corrected by fractionation equation as long as the recovery of Sr was up to 50%, but no one can doubt that
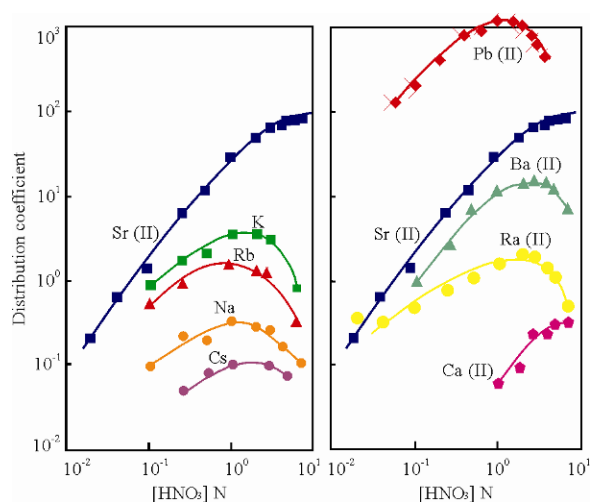
Figure. 4 Distribution coefficients of metal irons between nitric acid and Sr spec^TM resin(Philip Horwitz et al., 1992).
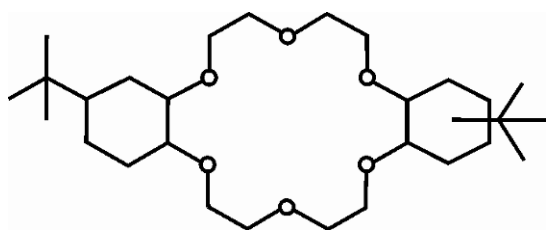

Figure. 5 Structure of Sr spec^TM resin.

enhancing recovery was still an important method to reduce isotopic fractionation. Acid eluent volume and resin mass can both influence the recovery (Scher et al., 2014; De Muynck et al., 2009). Charlier et al. (2006) proposed that Sr spec^TM resin was disposable, but De Muynck et al. (2009) had performed three times of regeneration experiments on Sr spec^TM resin by using 6 N HCl and deionized water, and accurate isotopic ratio with recovery of closed to 100% can be acquired when standard samples were separated by re-generated resin.

Commonly used micro-ion exchange column is made by micro-pasteurized pipette tips, although it can separate Sr from interference elements, but the challenge that recovery is low and resin is easy to spill from both sides of plug board should be faced. The Savillex micro-ion exchange column developed recently has overcame the drawbacks mentioned above. In addition, the micro-ion exchange column can also be customized in relevant website (http://www.mcmaster.com/#rods-(made-with-teflon-ptfe)/=qynbg8) according to experimental requirements. De Muynck et al. (2009) and Scher et al. (2014) studied the volume of ion exchange column and pointed out that although the separating column （1 ml） with large volume was beneficial to separating Sr from interfering elements, the high-amount of eluents would result in Ba mixed in Sr fraction and procedural blank increased. 125 μl micro- ion exchange columns can completely separate Ba from Sr and a small amount of eluents is also conducive to maintain a low procedural blank.

In order to facilitate observation and comparison, Table 2 summarizes different separation procedures of Sr when Sr spec^TM resin is used. Separation process consists of six steps: ① Elution of resin and ion exchange column; ② Balancing resin; ③ Adding sample solution in column; ④ Elution of interfering elements (Rb, Ca and Ba); ⑤ Elution and collection of Sr; ⑥ Resin regeneration.

3 SAMPLE LOADING AND MASS SPECTROMETRY
3.1 Sample Loading

Low ion production is an important factor to constrian the precise determination of the Sr isotope ratio in the samples with low Sr content, which indicates that the signal strength of samples may be lower than instrument detection limit and severe mass fractionation of isotope may occure in metal filament. When the samples with low Sr content are loaded in metal filament, the Sr ion production can be enhanced by improving the material (Li et al., 2005) and configuration of metal filament, melting Parafilm on both sides of metal filament in order to prevent sample from diffusion (Harlou et al., 2009; Font et al., 2007; Charlier et al., 2006), as well as adopting activators such as $TaF_5+H_3PO_4$ or $TaCl_5+H_3PO_4$ during TIMS analyses (Koornneef et al., 2013; Li et al., 2007).

Within thermal ionization source, atoms are adsorbed on the surface of metal band, and atoms will occure ionization due to Langmuir effect when the work function of metal filament (Ta filament: -4.25 eV; W filament: -4.58 eV; Re filament: -4.98 eV）is greater than the first ionization energy of analytical element. The higher the work function of metal filament is, the higher the ionization efficiency of analytical element is (Becker, 2008). When Sr isotope is analyzed, Ta filament is generally selected. However, the W filament and Re filament with high work function are recomonded when the samples with low Sr content are analyzed. For example, Li et al. (2005) performed condition experiments on Ta, Re and W metal filaments in Rb-Sr dating for single particles of mica.The results revealed that W filament is the optimum choice for sample loading. Krabbenhöft et al. (2009) selected Re single filament to measure Sr isotopic ratios of marine carbonates, water and hydrothermal fluids. The improvement on the configuration of metal filament, such as ship, pipe and V form, leads to the locations of samples concentrated. The improvement of metal filaments from single filament to dual filaments and tri-filaments can better control the evaporation and ionization of samples (Becker, 2008). All the methods mentioned above can improve ion production.

The usage and coating manner of activators will affect the stability and ion production of ion beam. Activator is porous, which can increase the contact area between measured elements and metal filaments and thereby improve ion production. $TaF_5/TaCl_5$ activator is commonly used to analyze Sr isotope (Koornneef et al., 2013). Harvey and Baxter (2009) found that ion production couldn't be improved if the mass of activator was too small. Nevertheless, the stability of the ion beam would be affected when the mass of activator was too large due to its uneven distribution on metal filament (Harvey and Baxter (2009). Moreover, they discovered that both the "activator+sample+activator" coating method and "activator+sample" coating method could improve ion production and they had similar efficiency. However, the ion production would not be increased but be restrained if sampes and activator were mixed evenly.
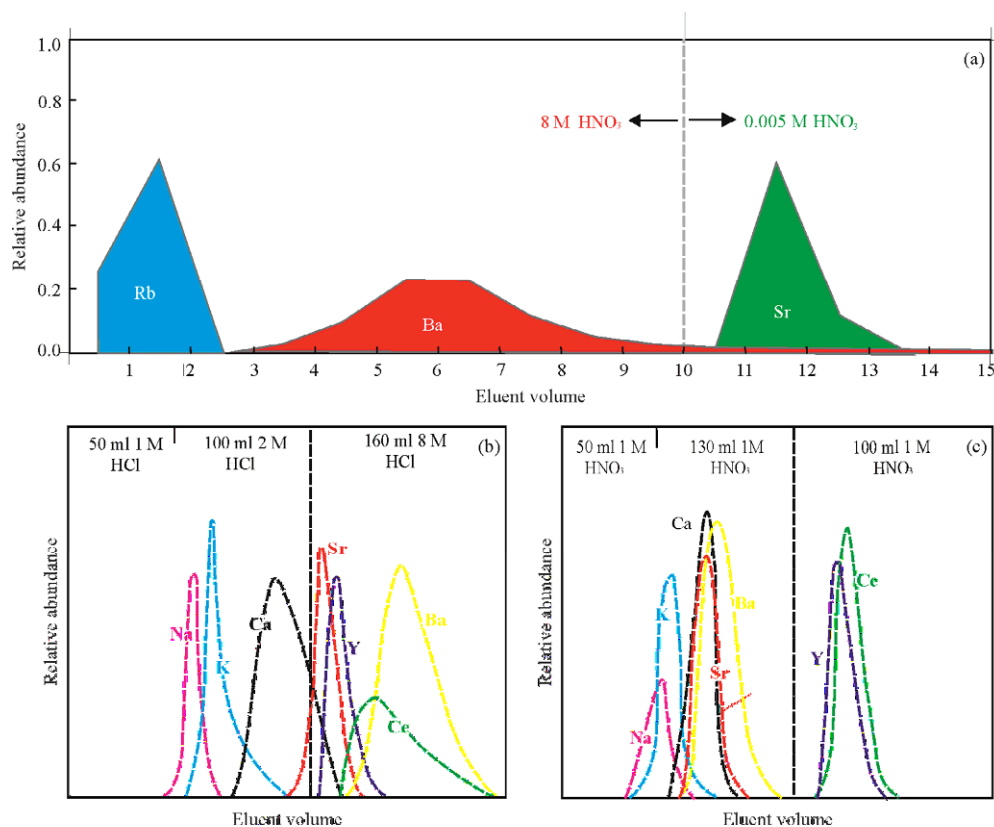
Figure. 6 The elution volume curves for Sr when the traditional resin, HCl (a) and HNO$_3$ (b) (after Dickin, 2005), as well as Sr spec^{TM} resin and HNO$_3$ (c) are used (after Scher et al., 2014).

3.2 Mass Spectrometry and Fractionation Correction

The Faraday cup configuration of Sr isotope ratio on TIMS is shown in Table 3. For the samples with low Sr content, relevant instrument components should be cleaned and baked before being analyzed. To some extent, cleaning ion lens and ion source is helpful for decreasing blank (Harlou et al., 2009). Baking ion source and the entire instrument under high temperature can make instrument maintain good vacuum degree and low instrument blank (Dos Santos et al., 2013).

For mass spectrometry, temperature program and the selection of integration time are also very important. Temperature program should not only assure the small amount of Rb burn out before Sr is analyzed, but also assure to obtain high-precision data as soon as possible. Font et al. (2007) and Harlou et al. (2009) adopted a rate of 50 mA / min to increase temperature until Rb disappeared (i.e., signal reduced to zero), and then performed blank deduction (about 30s) and gain correction. In addition, although the longer the integration time is, the higher the precision of the data is, most laboratories have lasted the integration time of 4s or 8s considering the practicability of this method and the small mass load of samples (Koornneef et al., 2013; Harlou et al., 2009; Font et al., 2007). Chu et al. (2006) and Charlier et al. (2006) considered that the use of virtual amplifier could eliminate the error of Faraday cup gain calibration and improve the accuracy of isotope ratio measurement and external reproducibility. But Harlou et al. (2009) considered virtual amplifier cannot improve the accuracy of isotope ratio and didn't recommend to use it. Virtual amplifier can change the feedback resistors through software automatically turn, then eliminate the differences between amplifiers after each detector acquires one group of data. When this function is used, the group number of data must be integer multiple of the number of Faraday cup.

For the mass fractionation correction of Sr isotope, power or exponential law and $^{86}Sr/^{88}Sr=0.119\ 4$ are generally used as internal standard (Darbyshire and Sewell, 1997). Different mass load of Sr element will result in different fractionation behavior. For the samples with low Sr content, the mass load is small and the analysis time is long. Hence, the fractionation is severe and poor in regularity (Fig. 7) (Harlou et al., 2009; Charlier et al., 2006) . Harlou et al. (2009) revealed that with the increase of analysis time, the $^{86}Sr/^{88}Sr$ value of the samples with high Sr content (6ng) would reduce to 0.119 4 systematically, but isotope fractionation would occur fast and $^{86}Sr/^{88}Sr$ value could be lower than 0.116 when the mass load of Sr isotope was 0.3 ng, $^{86}Sr/^{88}Sr$ value would fluctuate, higher or lower than 0.119 4 sometimes when the mass load of Sr isotope was 0.6 ng. Although the fractionation of the samples with low Sr content was severe and poor in regularity, it could still be corrected by the law of fractionation as a whole and exponential law was optimized (Harlou et al., 2009; Charlier et al., 2006). However, some challenges should be faced when $^{86}Sr/^{88}Sr=0.119\ 4$ was taken as internal standard to perform Sr isotope fractionation correction (Yang, 2009). The $^{86}Sr/^{88}Sr$ value of different natural samples may be different (Wei et al., 2013; Halicz et al., 2008) and sample separation by ion exchange can also generate significant mass fractionation. Therefore, a certain deviation may exist between the true $^{87}Sr/^{86}Sr$ value and the $^{87}Sr/^{86}Sr$ value

Table 2 Comparison of different separation procedures of Sr when Sr spec[TM] resin is used

Number	Sr isotope content (Procedural blank)	Separation procedure	Recovery	Reference	Note
1	0. 5 ng (6±1 pg)	① Washing resin with 6 N HCl and deionized water alternately; ② Balancing resin with 3 N HNO₃; ③ Adding sample solution with 3 N HNO₃ medium in column; ④ Washing interference element with 3 N HNO₃; ⑤ Leaching Sr with 0.05 N HNO₃ ⑥ Regenerating resin with 6 N HCl and deionized water	/	(Li et al., 2005)	
2	0.3–1 ng (11.7±3 pg)	① Washing resin with 6 N HCl and deionized water alternately; ② Balancing resin with (100*2) μl 3 N HNO₃; ③ Adding sample solution with 180 μl 3 N HNO₃ in column; ④ Washing interference element with 400 μl 3 N HNO₃ ⑤ Eluting Sr with (100+200) μl deionized water ⑥ Regenerating resin with 6 N HCl and deionized water	70%	(Harlou et al., 2009; Font et al., 2007; Charlier et al., 2006)	Separation is completed with 1.08 ml dissolution.
3	100 ng (40 pg)	① Washing resin with 6 N HCl and deionized water alternately; ② Balancing resin with 7 N HNO₃; ③ Adding sample solution with 7 N HNO₃ medium in column; ④ Washing interference element with 7 N HNO₃ ⑤ Eluting Sr with 0.05 N HNO₃ ⑥ Regenerating resin with 6 N HCl and deionized water	101.3%	(De Muynck et al., 2009)	Eluting Sr isotope in the samples with high Ca content using high concentrated HNO₃
4	2000 ng (160 pg)	① Connecting the syringe, micro-column and vacuum device, adding resin in column under a certain pressure ② Washing resin with 8 N HNO₃ and deionized water alternately; ③ Adjusting the pressure of vacuum apparatus with 8 N HNO₃ medium in order to keep flow rate ≤1 ml*min⁻¹ ; ④ Adding the sample solution with 0.25 ml 8 N HNO₃ medium in column; ⑤ Washing interference element with 3.5 ml 8 N HNO₃ ⑥ Eluting Sr with 4 ml deionized water	88%	(Wall et al., 2013)	Performing chemical separation with vacuum device

obtained through traditional analysis method that constant $^{86}Sr/^{88}Sr$ ratio was applied to correct mass value. However, how great this deviation has influenced geoscientific research is still needed to be further studied.

3.3 Instrumental Noise

The electronic noise of detectors (Faraday cup) can also affect the determination of the Sr isotope ratio in the samples with low Sr content (Koornneef et al., 2013; Wieser and Schwieters, 2005). Electronic noise may be described as follows:

$$\Delta V = \sqrt{\frac{4k_B R T}{t_m}}$$ （3.4）

Here, ΔV is electronic noise (V), k_B is Boltzmann constant (1.38×10⁻²³ J/K), R is amplifier resistivity (Ω), T is Kelvin temperature (K), t_m is integration time (s). The electronic noise of Faraday cup is related with resistivity, temperature and integration time of amplifier. Moreover, since the electronic noise of Faraday cup is positively related with the square root of the resistivity of amplifier, when the resistivity of amplifier expands 10 times, in theory, signal to noise ratio will increase √10 times. Large resistivity has significantly increased the

Table 3 Faraday cup configuration of Sr measured by TIMS

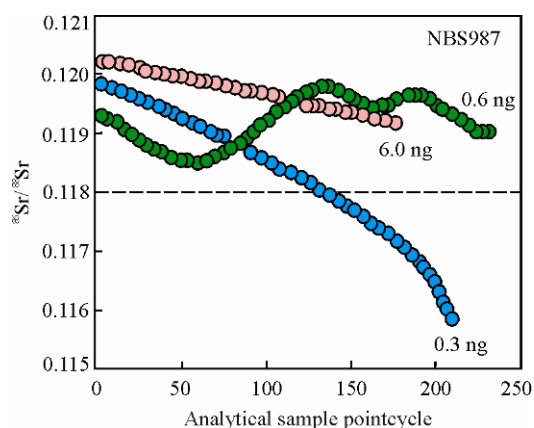| L4	L3	L2	L1	C	H1	H2	H3	H4
		^{84}Sr	^{85}Rb	^{86}Sr	^{87}Sr	^{88}Sr		

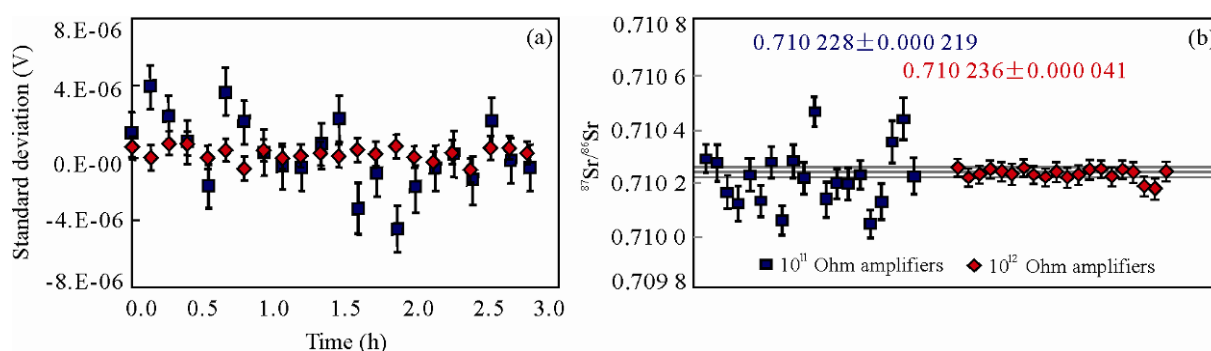**Figure. 7** Fractionation behavior of Sr when the Sr mass loaded is different (Harlou et al., 2009).

Figure. 8 (a) Reproducibility of 11 min baselines measured over 3h for $10^{11}\Omega$ and $10^{12}\Omega$ feedback resistors, that are 2.1 and 0.4 μv, respectively; (b) external reproducibility of multiple analyses of $^{87}Sr/^{86}Sr$ ratios at 20 mV ^{87}Sr beam intensity measured using 10^{11} Ω and 10^{12} Ω feedback resistors (Koornneef et al., 2013).

stability of background signal. For example, the electronic noise 1SD measured by Koornneef et al. (2013) was 2.1 μv and 0.4 μv when amplifier resistivity was $10^{11}\Omega$ and $10^{12}\Omega$, respectively (Fig. 8a). It should be pointed out that high resistivity can only improve the accuracy of the isotope ratio of the samples with low Sr content, but not contribute to the samples with high Sr content. For the samples with ^{87}Sr signal value of 20 mV, the $^{87}Sr/^{86}Sr$ external precision obtained from $10^{12}\Omega$ and $10^{11}\Omega$ resistivity was 58 ppm and 308 ppm, respectively, indicating that high resistivity has improved measurement precision by about 6 times (Fig. 8b). The use of $10^{12}\Omega$ can improve signal strength and signal to noise ratio, but the decay time of its signal will significantly increase. This problem can be solved through increasing the settling time/delay time of magnetic field (Koornneef et al., 2014; Koornneef et al., 2013). Furthermore, the stability of ion current is still

very important when high resistivity is used. High resistivity of $10^{13}\Omega$ has rapidly developed in recent years (Koornneef et al., 2015; Koornneef et al., 2014).

4 APPLICATION PROSPECT

Rb-Sr as one of the most classic isotopic systems has been widely applied to geochronology. The combination between ultra-low procedural blank chemical process and TIMS can be used to perform high-precise micro-analysis of the samples with ng magnitude, which can reflect the heterogeneity of internal minerals, construct the Rb-Sr isochore of internal monomineral as well as provide effective analytical testing method for the geochronological study of metamorphic rocks, dyke veins and tectonic rocks (Li et al., 2005). It has been successfully applied to study of evolution of magmatic system and Sr isotope measurement of monomineral such as plagioclase, K-feldspar and clinopyroxene (Zhu et al., 2013; Charlier et al., 2008). At present, this technique is also used to study the biological migratory path and breeding places (Font et al., 2012; Font et al., 2007). Meanwhile, it can also be used to analyze the Sr isotope compositions of precious samples. Therefore, the combination of ultra-low procedural blank and TIMS will be undoubtedly an important direction for Rb-Sr geochronology, geochemistry and environmental studies.

REFERENCES CITED

Arslan, Z., Secor, D. H., 2008. High Resolution Micromill Sampling for Analysis of Fish Otoliths by ICP-MS: Effects of Sampling and Specimen Preparation on Trace Element Fingerprints. *Marine Environmental Research*, 66(2008): 364–371

Barcikowski, S., Hahn, A., Kabashin, A. V., et al., 2007. Properties of Nanoparticles Generated during Femtosecond Laser Machining in Air and Water. *Applied Physics A*, 87(1): 47–55

Becker, S., 2008. Inorganic Mass Spectrometry: Principles and Applications. John Wiley & Sons

Besner, S., Kabashin, A. V., Meunier, M., 2007. Two-Step Femtosecond Laser Ablation-Based Method for the Synthesis of Stable and Ultra-Pure Gold Nanoparticles in Water. *Applied Physics A*, 88(2): 269–272

Boer, R., Beukes, G., Meyer, F., et al., 1993. Fluoride Precipitates in Silicate Wet-Chemistry: Implications on REE Fractionation. *Chemical geology*, 104(1): 93–98

Charlier, B. L., Wilson, C. J., Davidson, J. P., 2008. Rapid Open-System Assembly of a Large Silicic Magma Body: Time-Resolved Evidence from Cored Plagioclase Crystals in the Oruanui Eruption Deposits, New Zealand. *Contributions to Mineralogy and Petrology*, 156(6): 799–813

Charlier, B. L. A., Ginibre, C., Morgan, D., et al., 2006. Methods for the Microsampling and High-Precision Analysis of Strontium and Rubidium Isotopes at Single Crystal Scale for Petrological and Geochronological Applications. *Chemical Geology*, 232(3): 114–133

Chen, Z. H., Li, C., Qu, W. J. et al., 2010. Research and Preliminary Application in Metallogenic Chronology of Re-Os Isotope System in Graphite Samples. *Acta Petrologica Sinica*, 26(11): 3411–3417 (in Chinese with English Abstract)

Chu, Z. Y., Chen, F. K., Yang, Y. H. et al., 2009. Precise Determination of Sm, Nd Concentrations and Nd Isotopic Compositions at the Nanogram Level in Geological Samples by Thermal Ionization Mass Spectrometry. *Journal of Analytical Atomic Spectrometry*, 24(11): 1534–1544

Chu, Z. Y., Yang, Y. H., Qiao, G. S., 2006. A Calculation Method to Eliminate Gain Effect on Isotopic Measurement Using the Virtual Amplifier Multi-Collector Mass Spectrometer. *International Journal of Mass Spectrometry*, 253(1): 130–135

Claverie, F., Malherbe, J., Bier, N., et al., 2013. Standard Addition Method for Laser Ablation ICPMS Using a Spinning Platform. *Analytical Chemistry*, 85(7): 3584–3591

Cotta, A.J., Enzweiler, J., 2012. Classical and New Procedures of Whole Rock Dissolution for Trace Element Determination by ICP-MS. *Geostandards and Geoanalytical Research*, 36(1): 27–50

Darbyshire, D. P. F., Sewell, R. J., 1997. Nd and Sr Isotope Geochemistry of Plutonic Rocks from Hong Kong: Implications for Granite Petrogenesis, Regional Structure and Crustal Evolution. *Chemical Geology*, 143(1): 81–93

De Muynck, D., Huelga-Suarez, G., Van Heghe, L., et al., 2009. Systematic Evaluation of AStrontium-Specific Extraction Chromatographic Resin for Obtaining APurified Sr Fraction with Quantitative Recovery from Complex and Ca-Rich Matrices. *Journal of Analytical Atomic Spectrometry*, 24(11): 1498–1510

Deniel, C., Pin, C., 2001. Single-Stage Method for the Simultaneous Isolation of Lead and Strontium from Silicate Samples for Isotopic Measurements. *Analytica Chimica Acta*, 426(1): 95–103

Dickin, A. P., 2005. Radiogenic Isotope Geology. Cambridge University Press.

Dos Santos, M. E., Palmieri, H. E. L., Moreira, R.M., 2013. Testing the ^{87}Sr/^{86}Sr Isotopic Ratio Measured by ICP-MS as ATracer for Inter-Well Investigation in Oil Reservoirs, EPJ Web of Conferences. EDP Sciences. 204

Dulski, P., 2001. Reference Materials for Geochemical Studies: New Analytical Data by ICP-MS and Critical Discussion of Reference Values. *Geostandards Newsletter*, 25(1): 87–125

Font, L., Nowell, G. M., Pearson, D. G., et al., 2007. Sr Isotope Analysis of Bird Feathers by TIMS: ATool to Trace Bird Migration Paths and Breeding Sites. *Journal of Analytical Atomic Spectrometry*, 22(5): 513–522

Font, L., van der Peijl, G., van Wetten, I., et al., 2012. Strontium and Lead Isotope Ratios in Human Hair: Investigating APotential Tool for Determining Recent Human Geographical Movements. *Journal of Analytical Atomic Spectrometry*, 27(5): 719–732

Fortunato, G., Mumic, K., Wunderli, S., et al., 2004. Application of Strontium Isotope Abundance Ratios Measured by MC-ICP-MS for Food Authentication. J*ournal of Analytical Atomic Spectrometry*, 19(2): 227–234

Galler, P., Limbeck, A., Boulyga, S. F., et al., 2007. Development of An On-Line flow Injection Sr/Matrix Separation Method for Accurate, High-Throughput Determination of Sr Isotope Ratios by Multiple Collector-Inductively Coupled Plasma-Mass Spectrometry. *Analytical chemistry*, 79(13): 5023–5029

Halicz, L., Segal, I., Fruchter, N., et al., 2008. Strontium Stable Isotopes Fractionate in the Soil Environments? *Earth and Planetary Science Letters*, 272(1): 406–411

Harlou, R., Pearson, D. G., Nowell, G.M. et al., 2009. Combined Sr Isotope and Trace Element Analysis of Melt Inclusions at Sub-Ng Levels Using Micro-Milling, TIMS and ICPMS. *Chemical Geology*, 260(3): 254–268

Harvey, J., Baxter, E. F., 2009. An Improved Method for TIMS High Precision Neodymium Isotope Analysis of Very Small Aliquots (1–10 ng). *Chemical Geology*, 258(3): 251–257

Hayes, J. M., 1983. Practice and Principles of Isotopic Measurements in Organic Geochemistry. Organic Geochemistry of Contemporaneous and Ancient Sediments, 5: e5

Hinn, G. M., Nelson, B. K., 1997. Production and Analysis of Repetitive Sub-Boiling Laboratory Reagents for Purity Enhancement. Nuclear Instruments and Methods in Physics Research Section A: Accelerators, Spectrometers, *Detectors and Associated Equipment,* 397(1997): 189–193

Hoffmann, D. L., Spötl, C., Mangini, A., 2009. Micromill and in Situ Laser Ablation Sampling Techniques for High Spatial Resolution MC-ICPMS U-Th Dating of Carbonates. *Chemical Geology*, 259(2009): 253–261

Hu, Z. C., Gao, S., Hu, S. H., et al., 2005. Suppression of Interferences for Direct Determination of Arsenic in Geological Samples by Inductively Coupled Plasma Mass Spectrometry. *Journal of Analytical Atomic Spectrometry*, 20(11): 1263–1269

Hu, Z.C., Gao, S., Liu, Y. S., et al., 2010. NH$_4$F Assisted High Pressure Digestion of Geological Samples for Multi-Element Analysis by ICP-MS. *Journal of Analytical Atomic Spectrometry*, 25(3): 408–413

Hu, Z. C., Liu, Y. S., Gao, S., et al., 2012. Improved in Situ Hf Isotope Ratio Analysis of Zircon Using Newly Designed X

Skimmer Cone and Jet Sample Cone in Combination with the Addition of Nitrogen by Laser Ablation Multiple Collector ICP-MS. *Journal of Analytical Atomic Spectrometry*, 27(9): 1391–1399

Hu, Z. C., Qi, L., 2014. 15.5-Sample Digestion Methods. In: Turekian, H. D. H. K. ed., Treatise on Geochemistry (Second Edition). Elsevier, Oxford, 87–109

Hwang, J., Druffel, E. R. M., 2008. Blank Correction for Delta C-14 Measurements in Organic Compound Classes of Oceanic Particulate Matter. *Radiocarbon*, 47(1): 75–87

Jackson, S. E., Longerich, H. P., Dunning, G. R., et al., 1992. The Application of Laser-Ablation Microprobe-Inductively Coupled Plasma-Mass Spectrometry (LAM-ICP-MS) to in Situ Trace-Element Determinations in Minerals. *Canadian Mineralogist*, 30(1992): 1049–1049

Jarvis, K. E., 1990. A Critical Evaluation of Two Sample Preparation Techniques for Low-Level Determination of some Geologically Incompatible Elements by Inductively Coupled Plasma-Mass Spectrometry. *Chemical Geology*, 83(1): 89–103

Jochum, K., Stoll, B., Weis, U., et al., 2009. In Situ Sr Isotopic Analysis of Low Sr Silicates Using LA-ICP-MS. *Journal of Analytical Atomic Spectrometry*, 24(9): 1237–1243

Kabashin, A. V., Meunier, M., 2007. Femtosecond Laser Ablation in Aqueous Solutions: ANovel Method to Synthesize Non-Toxic Metal Colloids with Controllable Size. *Journal of Physics*: *Conference Series. IOP Publishing*, 354

Kimura, J. I., Takahashi, T., Chang, Q., 2013. A NewAnalytical Bias Correction for in Situ Sr Isotope Analysis of Plagioclase Crystals Using Laser-Ablation Multiple-Collector Inductively Coupled Plasma Mass Spectrometry. *Journal of Analytical Atomic Spectrometry*, 28(6): 945–957

Komárek, M., Ettler, V., Chrastný, V., et al., 2008. Lead Isotopes in Environmental Sciences: A Review. *Environment International*, 34(4): 562–577

Konter, J. G., Storm, L. P., 2014. High Precision $^{87}Sr/^{86}Sr$ Measurements by MC-ICP-MS, Simultaneously Solving for Kr Interferences and Mass-Based Fractionation. *Chemical Geology*, 385(2014): 26–34

Koornneef, J., Bouman, C., Schwieters, J., et al., 2014. Measurement of Small Ion Beams by Thermal Ionisation Mass Spectrometry Using New 10^{13} Ohm Resistors. *Analytica Chimica Acta*, 819(2014): 49–55

Koornneef, J. M., Bouman, C., Schwieters, J. B., et al., 2013. Use of 10^{12}Ohm Current Amplifiers in Sr and Nd Isotope Analyses by TIMS for Application to Sub-Nanogram Aamples. *J. Anal. At. Spectrom.*, 28(5): 749–754

Koornneef, J. M., Nikogosian, I., van Bergen, M. J., et al., 2015. TIMS Analysis of Sr and Nd Isotopes in Melt Inclusions from Italian Potassium-Rich Lavas Using Prototype 10^{13} Ohm Amplifiers. *Chemical Geology*, 397(2015): 14–23

Košler, J., Magna, T., 2014. 15.6-Developments in Clean Lab Practices. In: Turekian, H. D. H. K., ed., Treatise on Geochemistry (Second Edition). Elsevier, Oxford. 111–122

Krabbenhöft, A., Fietzke, J., Eisenhauer, A., et al., 2009. Determination of Radiogenic and Stable Strontium Isotope Ratios ($^{87}Sr/^{86}Sr$; $\delta^{88}/^{86}Sr$) by Thermal Ionization Mass Spectrometry Applying An$^{87}Sr/^{84}Sr$ Double Spike. *Journal of Analytical Atomic Spectrometry*, 24(9): 1267–1271

Kuehner, E. C., Alvarez, R., Paulsen, P. J., et al., 1972. Production and Analysis of Special High-Purity Acids Purified by Subboiling Distillation. *Analytical Chemistry*, 44(12): 2050–2056

Langmyhr, F., 1967. The Removal of Hydrofluoric Acid by Evaporation in the Presence of Sulfuric or Perchloric Acids. *Analytica Chimica Acta*, 39(1967): 516–518

Li, C.F., Chen, F. K., Li, X. H., 2007. Precise Isotopic Measurements of Sub-Nanogram Nd of Standard Reference Material by Thermal Ionization Mass Spectrometry Using the NdO$^+$ Technique. *International Journal of Mass Spectrometry*, 266(1): 34–41

Li, C. F., Guo, J. H., Yang, Y. H., et al., 2011. Single-Step Separation of Rb-Sr and Pb from Minor Rock Samples and High Precision Determination Using Thermal Ionization Mmass Spectrometry. *Geochimica*, 40(5): 399–406, (in Chinese with English Abstract)

Li, C. F., Li, X. H., Li, Q. L., et al., 2012. Rapid and Precise Determination of Sr and Nd Isotopic Ratios in Geological Samples from the Same Filament Loading by Thermal Ionization Mass Spectrometry Employing A Single-Step Separation Scheme. *Analytica Chimica Acta*, 727(5): 54–60

Li, Q. L., Chen, F. K., Wang, X. L. et al., 2005. Ultra-Low Procedural Blank and the Single-Grain Mica Rb-Sr Isochron Dating. *Chinese Science Bulletin*, 50(24): 2861–2865

Lin, L., Hu, Z. C., Yang, L. et al., 2014. Determination of Boron Isotope Compositions of Geological Materials by Laser Ablation MC-ICP-MS Using Newly Designed High Sensitivity Skimmer and Sample cones. *Chemical Geology*, 386(2014): 22–30

Liu, Y. S., Hu, Z. C., Li, M., et al., 2013. Applications of LA-ICP-MS in the Elemental Analyses of Geological Samples. *Chinese Science Bulletin*, 58(32): 3863–3878

Müller, W., Aerden, D., Halliday, A.N., 2000a. Isotopic Dating of Strain Fringe Increments: Duration and Rates of Deformation in Shear Zones. *Science*, 288(5474): 2195–2198

Müller, W., Mancktelow, N.S., Meier, M., 2000b. Rb–Sr Microchrons of Synkinematic Mica in Mylonites: An Example from the DAV fault of the Eastern Alps. *Earth and Planetary Science Letters*, 180(3): 385–397

Mank, A. J. G., Mason, P. R. D., 1999. A Critical Assessment of Laser Ablation ICP-MS as An Analytical Tool for Depth Analysis in Silica-Bbased Glass Samples. *Journal of Analytical Atomic Spectrometry*, 14(8): 1143–1153

Mariet, C., Belhadj, O., Leroy, S. et al., 2008. Relevance of NH$_4$F in Acid Digestion before ICP-MS Analysis. *Talanta*, 77(1): 445–450

Maxwell, S. L., Culligan, B. K., 2009. Rapid Method for Determination of Radiostrontium in Emergency Milk Samples. *Journal of Radioanalytical and Nuclear Chemistry*, 279(3): 757–760

Moody, J. R., Lindstrom, R. M., 1977. Selection and Cleaning

of Plastic Containers for Storage of Trace Element Samples. *Analytical Chemistry*, 49(14): 2264–2267

Na, C. K., Nakano, T., Tazawa, K. et al., 1995. A Systematic and Practical Method of Liquid Chromatography for the Determination of Sr and Nd Isotopic Ratios and REE Concentrations in Geological Samples. *Chemical Geology*, 123(1): 225–237

Navarro, M. S., Andrade, S., Ulbrich, H. et al., 2008. The Direct Determination of Rare Earth Elements in Basaltic and Related Rocks using ICP-MS: Testing the Efficiency of Microwave Oven Sample Decomposition Procedures. *Geostandards and Geoanalytical Research*, 32(2): 167–180

Okabayashi, S., Yokoyama, T. D., Kon, Y. et al., 2011. Evaluation of Laser Ablation in Liquid (LAL) Technique as a New Sampling Technique for Elemental and Isotopic Analysis Using ICP-Mass Spectrometry. *Journal of Analytical Atomic Spectrometry*, 26(7): 1393–1400.

Palmer, J. S., Duffy, D. L., Box, N. F. et al., 2000. Melanocortin-1 Receptor Polymorphisms and Risk of Melanoma: Is the Association Explained Solely by Pigmentation Phenotype? *The American Journal of Human Genetics*, 66(1): 176–186

Philip Horwitz, E., Chiarizia, R., Dietz, M.L., 1992. A Novel Strontium-Selective Extraction Chromatographic Resin. *Solvent Extraction and Ion Exchange*, 10(2): 313–336

Raczek, I., Jochum, K. P., Hofmann, A. W., 2003. Neodymium and Strontium Isotope Data for USGS Reference Materials BCR-1, BCR-2, BHVO-1, BHVO-2, AGV-1, AGV-2, GSP-1, GSP-2 and Eight MPI-DING Reference Glasses. *Geostandards Newsletter*, 27(2): 173–179

Raddatz, J., Liebetrau, V., Rüggeberg, A. et al., 2013. Stable Sr-Isotope, Sr/Ca, Mg/Ca, Li/Ca and Mg/Li Ratios in the Scleractinian Cold-Water Coral Lophelia Pertusa. *Chemical Geology*, 352(2013): 143–152

Reimann, C., Birke, M., Filzmoser, P., 2010. Bottled Drinking Water: Water Contamination from Bottle Materials (Glass, Hard PET, Soft PET), the Influence of Colour and Acidification. *Applied Geochemistry*, 25(7): 1030–1046

Scher, H. D., Griffith, E. M., Buckley, W. P., 2014. Accuracy and Precision of $^{88}Sr/^{86}Sr$ and $^{87}Sr/^{86}Sr$ Measurements by MC-ICP-MS Compromised by High Barium Concentrations. *Geochemistry, Geophysics, Geosystems*, 15(2): 499–508

Tong, J. G., Li, S. R., Li, X. H. et al., 2006. Determination on $^{87}Sr/^{86}Sr$ Ratio and Stratigraphic Dating of Single-Grain Foraminifera. *Chinese Science Bulletin*, 51(17): 2141–2145

Waight, T., Baker, J., Peate, D., 2002. Sr Isotope Ratio Measurements by Double-Focusing MC-ICPMS: Techniques, Observations and Pitfalls. *International Journal of Mass Spectrometry*, 221(3): 229–244

Wall, A. J., Capo, R., Stewart, B. et al., 2013. High throughput Method for Sr Extraction from Variable Matrix Waters and $^{87}Sr/^{86}Sr$ Isotope Analysis by MC-ICP-MS. *Journal of Analytical Atomic Spectrometry*, 28(8): 1338–1344

Wei, G. J., Ma, J. L., Liu, Y. et al., 2013. Seasonal Changes in the Radiogenic and Stable Strontium Isotopic Composition of Xijiang River Water: Implications for Chemical Weathering. *Chemical Geology*, 343(2013): 67–75

Wieser, M. E., Schwieters, J. B., 2005. The Development of Multiple Collector Mass Spectrometry for Isotope Ratio Measurements. *International Journal of Mass Spectrometry*, 242(2): 97–115

Yang, L., 2009. Accurate and Precise Determination of Isotopic Ratios by MC-ICP-MS: A Review. *Mass Spectrometry Reviews*, 28(6): 990–1011

Yokoyama, T., Makishima, A., Nakamura, E., 1999. Evaluation of the Coprecipitation of Incompatible Trace Elements with Fluoride during Silicate Rock Dissolution by Acid Digestion. *Chemical Geology*, 157(3): 175–187

Yokoyama, T., Nakamura, E., 2004. Precise Analysis of the $^{228}Ra/^{226}Ra$ Isotope Ratio for Short-Lived U-Series Disequilibria in Natural Samples by Total Evaporation Thermal Ionization Mass Spectrometry (TE-TIMS). *Journal of Analytical Atomic Spectrometry*, 19(6): 717–727

Yuan, H. L., Hu, S. H., Tong, J. et al., 2000. Preparation of Ultra-Pure Water and Acids and Investigation of Background of An ICP-MS Laboratory. *Talanta*, 52(6): 971–981

Zhang, W., Hu, Z. C., Liu, Y. S. et al., 2012. Total Rock Dissolution Using Ammonium Bifluoride (NH_4HF_2) in Screw-Top Teflon Vials: A New Development in Open-Vessel Digestion. *Analytical Chemistry*, 84(24): 10686–10693

Zhu, X. Y., Chen, F. K., Liu, B. X. et al., 2013. Zircon U-Pb and K-Feldspar Megacryst Rb–Sr Isotopic Ages and Sr-Hf Isotopic Composition of the Mesozoic Heyu Pluton, Eastern Qingling Orogen, China. *Lithos*, 156: 31–40